

## Convective variability in the North American Monsoon using cloud-to-ground lightning data and high-resolution satellite precipitation data

Stephen W. Nesbitt<sup>1</sup> and Roger A. Akers, Jr.  
Department of Atmospheric Sciences  
University of Illinois, Urbana, IL

### Introduction

This study examines diurnal to intraseasonal variability in lightning characteristics of the North American Monsoon (NAM) using 5 years (2004-2008) of Vaisala's Long Range Lightning Detection Network (LLDN). The high-time and space resolution, as well as the continuous observation record of LLDN lightning data allows an unprecedented depiction of the diurnal cycle of cloud-to-ground lightning flash rates, and illustrates the coupling with topography and evolution of storms producing lightning in the North American Monsoon. Along with the NALDN data, this study also examines high-resolution satellite precipitation data from NOAA's Climate Prediction Center Morphing (CMORPH) rainfall estimates to examine variations in lightning-rainfall relationships and climatological radar echo vertical structure to infer the characteristics of convective systems.

### Data and Methods

Cloud to ground lightning flash locations were obtained from the Long-range Lightning Detection Network (LLDN), operated by Vaisala, Inc. (Murphy et al. 2006). The LLDN operates by detecting the distance and time of arrival of very low frequency (VLF) signals. In comparing satellite optically-detected flashes and LLDN detected flashes, Cummins et al. (1998) and Murphy and Holle (2005) described a method for determining the detection efficiency of the network outside the periphery of the NALDN network. The latter study showed that the region of northwest Mexico falls within a region of detectability by the NALDN. Using this technique Cramer and Cummins (1999) showed that the median location accuracy for flashes was 5 km over propagation lengths of 1200-1600 km.

LLDN detected flashes from ranges outside the line of sight of the sensors are VLF signals reflected within the earth-ionosphere waveguide. The ionospheric D-Layer has variable reflection height and sharpness depending on the time of day, varying depending on whether it is day or night. Flashes were corrected for detection efficiency (DE) using the day/night DE model of Pessi et al. (2009). The day/night terminator was projected upon the data to select the appropriate DE model depending on the local solar time (LST) of each detected flash occurrence. After the appropriate DE model was selected, flash counts were corrected by dividing the total number of day and night flashes by the fractional DE.

LLDN CG flash data from Vaisala were analyzed for the period June-September 2004-2008, following the NLDN network upgrade in early 2004. To compare the diurnal cycle of CG lightning and rainfall, CMORPH rainfall data (obtained from NOAA's Climate Diagnostics Center), described in Joyce et al. (2004), were analyzed over the same period as the LLDN data. CMORPH combines passive microwave rainfall estimates and "morphs" intermittent satellite overpasses using motion vectors from IR cloud tracking. Gochis et al. (2009) demonstrated the fidelity of CMORPH to depict rainfall over the NAM region. The data are given at 3 hourly (UTC), 0.25° resolution. This data was interpolated to local solar time with trigonometric interpolation using a discrete Fourier transform.

### Lightning Flash Rate Climatology over the NAM domain

Figure 1 shows the raw and DE-corrected lightning flash rate climatology in areas where the daytime DE is greater than or equal to 5%. This figure shows that Florida and northwest Cuba may contain comparable flash densities which are the highest in the domain. Within the core NAM region of northwest Mexico, corrected flash rates of  $> 15 \text{ fl}/(\text{km}^2 \text{ yr})$  are found within the northern Sierra Madre Occidental and

---

<sup>1</sup> Corresponding author e-mail: [snesbitt@illinois.edu](mailto:snesbitt@illinois.edu)

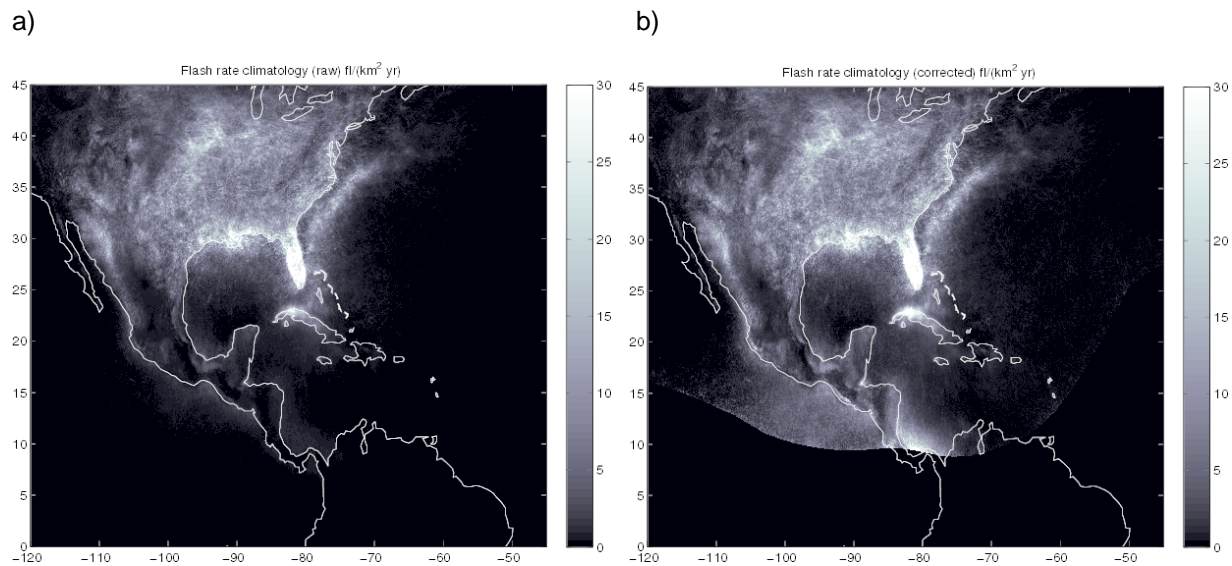


Figure 1. (a) Raw and (b) detection-efficiency corrected flash density ( $\text{fl}/(\text{km}^2 \text{ yr})$ ) climatology for June-September 2004-2008.

Mogollon Rim, with lower flash rates on the western slopes of the Sierra Madre Occidental south of  $25^\circ$  latitude. This is despite a rainfall gradient that is directed in the opposite zonal direction in this region. Further study is necessary to determine possible cloud microphysical differences or storm occurrence frequency differences which lead to this marked difference in lightning and rainfall production.

Murphy and Holle (2005) estimated that flash rates in the northern SMO may meet or exceed those observed in the US lightning maximum in Florida. We do not find that to be the case in this study, but this discrepancy may be a result of differing periods of analysis, changes in the characteristics of the NDLN, or differences in the DE model used.

### Diurnal Cycle of Lightning Activity

Fig. 2 shows the first diurnal Fourier harmonic of JJAS 2004-2008 DE-corrected lightning flash density over the core NAM domain, gridded at  $0.05^\circ$  resolution. The first Fourier harmonic captures much of the variance of the diurnal cycle of CG flashes in this domain, except notably over the region from Missouri to the Big Bend area of Texas, where double nocturnal-afternoon peak in CG activity is present (not shown). Over high terrain in the Rockies, Sierra Madre Occidental and Oriental, and most of Baja California there is an early to mid-afternoon peak in CG flash rates, while lower elevation regions surrounding these regions (except over Baja) see an evening-nighttime maximum in CG flash rates. The progression of phase in the rainfall diurnal cycle east of the Rockies has been studied by many (Tripoli and Cotton 1986; Carbone et al. 2002), while the progression from an afternoon to evening maximum along the western slopes of the SMO has been studied more recently by Lang et al. (2007) and Nesbitt et al. (2008). A sequence going from from a nocturnal to early-morning maximum in flash rate occurs off the west coast of Mexico, which differs in phase from the late morning maximum over the Gulf of Mexico. Note the high amplitude midnight maximum of CG lightning in the near-shore region from Puerto Vallarta north to Mazatlán.

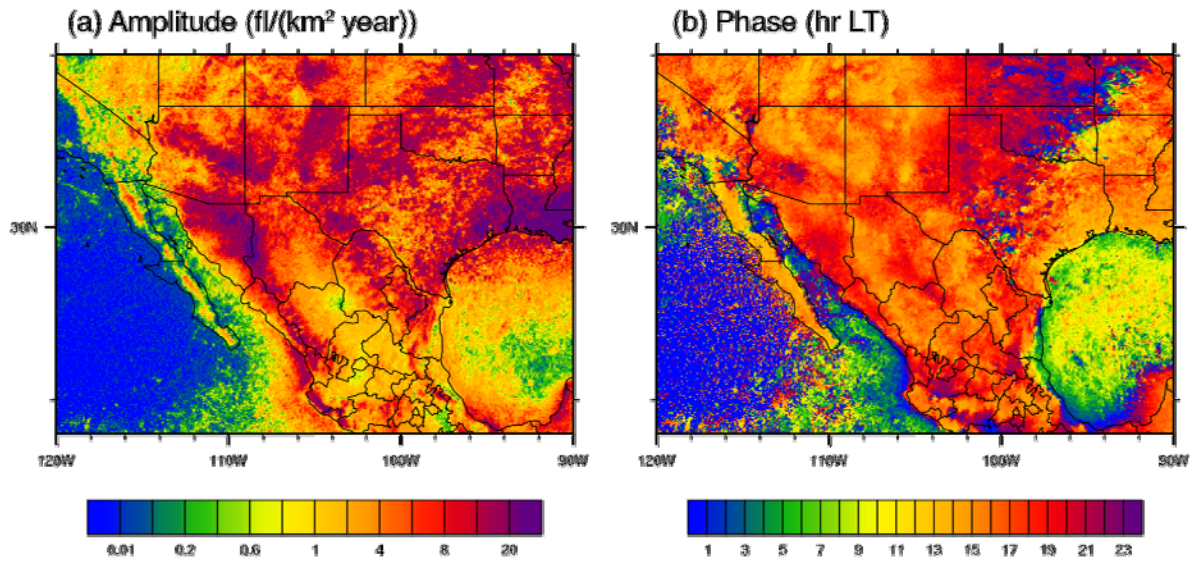


Fig. 2: (a) Amplitude (fl/(km<sup>2</sup> year)) and (b) phase (hours LT) of the first diurnal harmonic of JJAS 2004-2008 LLDN flashes.

### Diurnal Cycle Lightning and Rainfall Regimes in the North American Monsoon Region

To objectively identify diurnal cycle regimes in the NAM region using LLDN and CMORPH rainfall data, Empirical Orthogonal Functions (EOFs) with VARIMAX rotation are used. EOFs are rotated since there is no desired requirement for the EOFs to be orthogonal for the study of the diurnal cycle. LLDN and CMORPH data were gridded in 3 hr local time bins at 0.25° resolution for this study. The percent of variance explained by the first seven generated EOFs are presented in Figure 3 (along with sampling

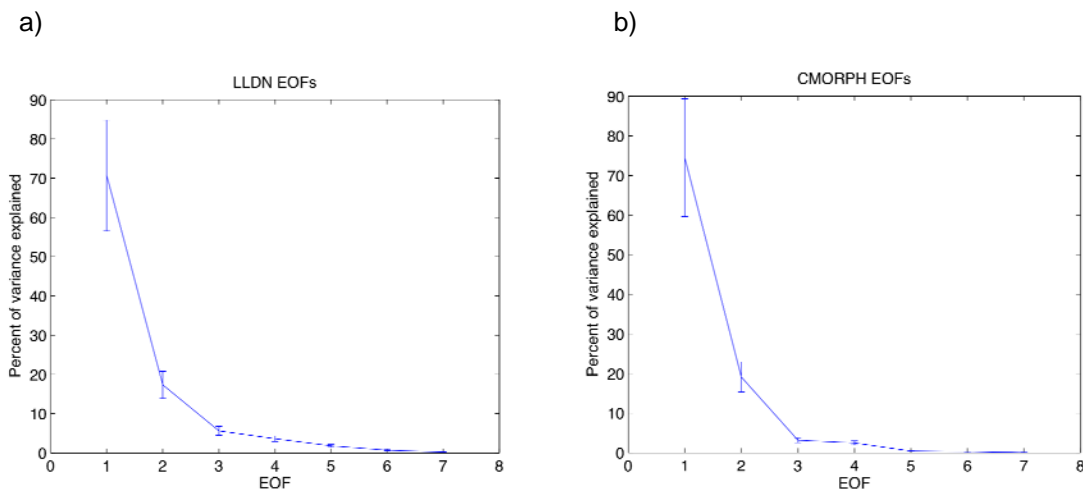


Fig. 3: Percent of variance explained by the first 7 EOF modes for the JJAS 2004-2008 diurnal cycle composites for the (a) LLDN and (b) CMORPH data.

error estimates according to North's rule of thumb; North et al. 1982) for both the LLDN and CMORPH composites. The figures show that the percent of variance explained by both the LLDN and CMORPH first EOFs explain more than 70 percent of the variance in the composites, while the second EOFs explain nearly 20 percent. The third and fourth EOFs explain similar fractions of EOFs (and may not be considered statistically different from each other, but are clearly separated in terms of significance from the fifth and higher EOFs. Henceforth, we choose to examine the first through the fourth EOFs because of their separation from the remainder of the EOFs.

Figure 4 shows the normalized spatial patterns (loadings) and time series of the first four EOFs of the composite LLDN and CMORPH diurnal composites. The EOF spatial patterns for both the LLDN and CMORPH EOF 1s display a pattern of an afternoon maximum/afternoon in CG lightning and rainfall over the SMO, although the rainfall peak occurs one bin (3 hr) later than the lightning peak. This may be due to the fact that stratiform rain produced by mesoscale convective systems (MCSs) likely delays the rainfall peak past the convective rainfall peak in mid-afternoon (Nesbitt and Zipser 2003). Additionally, there is no signal in rainfall in EOF 1 over the mountains in the SW US. EOF 2 patterns and time series are more similar than for EOF 1, with the time series being almost relatively identical (although the sign is arbitrarily reversed). EOF 3 differs among the two composites, with the LLDN EOF 2 detecting a noon-time

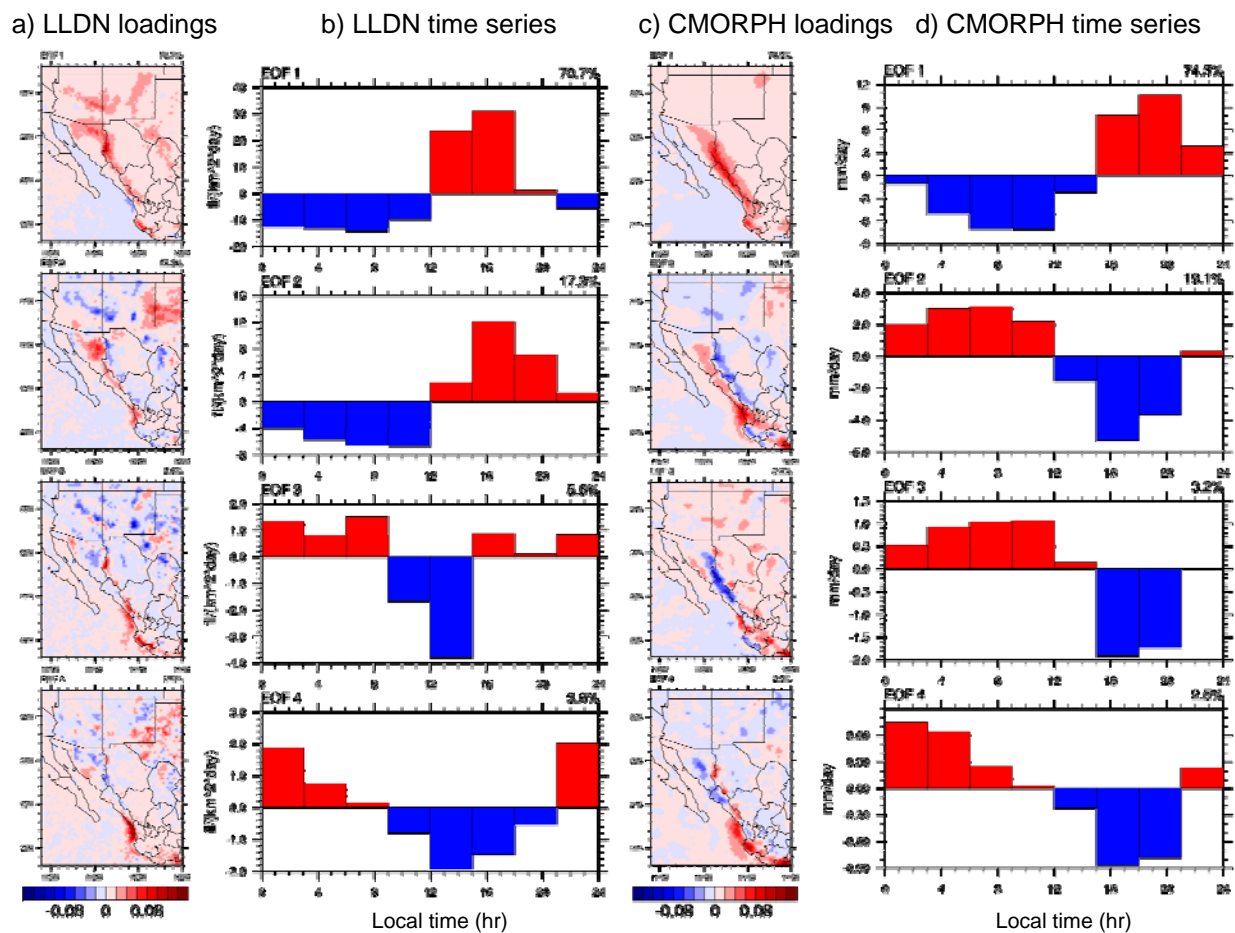


Fig. 4. EOF loadings (normalized, a,c) and time series (in data units, b,d) for the LLDN JJAS 2004-2006 LLDN (a,b) and CMORPH (c,d) diurnal composites.

maximum in the SW US/noon-time minimum offshore of Mexico south of Mazatlan, while the CMORPH rainfall EOF 3 picks up a strong afternoon maximum over the western slopes of the SMO/nocturnal minimum over the terrain in the SW US. EOF 4 becomes more similar, with both LLDN and CMORPH EOF 4s picking up the midnight maximum offshore of Mexico.

## Conclusions

This study demonstrates the capability of DE-corrected Vaisala LLDN in depicting the diurnal cycle of convection in the NAM domain. The high effective resolution of lightning composites allows the dependence of the diurnal cycle on terrain elevation to be elucidated. Comparisons of CG lightning flash rates and satellite rainfall estimates provided by CMORPH show close correspondence in their depiction of the diurnal cycle. Future study will examine the space-time variation of the diurnal cycle and its relation to synoptic to intraseasonal variability within the NAM.

*Acknowledgements.* Funding for this project was provided by the NOAA CPPA program.

## References

- Carbone, R. E., J. D. Tuttle, D. A. Ahijevych, and S. B. Trier, 2002: Inferences of predictability associated with warm season precipitation episodes. *J. Atmos. Sci.*, **59**, 2033-2056.
- Cummins, K. L., M. J. Murphy, E. A. Bardo, W. L. Hiscox, R. D. Pyle, and A. E. Pifer, 1998: A combined TOA/MDF technology upgrade of the U.S. National Lightning Detection Network. *J. Geophys. Res.*, **103**, 9035–9044.
- Lang, T. J., D. Ahijevych, S. W. Nesbitt, R. Carbone, and S. A. Rutledge, 2007: Radar-observed characteristics of precipitating systems during NAME 2004. *J. Climate*, **20**, 1713-1733.
- Murphy, M.J., and R.L. Holle, 2005: Where is the real cloud-to-ground lightning maximum in North America? *Wea. Forecasting*, **20**, 125–133.
- Murphy, M. J., N. W. S. Demetriades, R. L. Holle and K. L. Cummins, 2006: Overview of capabilities and performance of the U.S. National Lightning Detection Network. Preprints, *Second Conference on the Meteorological Applications of Lightning Data*, American Meteorological Society, Atlanta, GA, 30 January–2 February 2006.
- Nesbitt, S. W., and E. J. Zipser, 2003: The diurnal cycle of rainfall and convective intensity according to three years of TRMM measurements. *J. Climate*, **16**, 1456-1475.
- Nesbitt, S. W., D. J. Gochis, and T. J. Lang, 2008: The diurnal cycle of clouds and precipitation along the Sierra Madre Occidental during the North American Monsoon Experiment: Implications for precipitation estimation in complex terrain. *J. Hydromet.*, **9**, 728-743.
- North G. R., T. L. Bell, R. F. Cahalan, and F. J. Moenig, 1982: Sampling errors in the estimation of empirical orthogonal functions. *Mon. Wea. Rev.*, **110**, 669–706.
- Pessi, A.T., S. Businger, K.L. Cummins, N.W.S. Demetriades, M. Murphy, and B. Pifer, 2009: Development of a long-range lightning detection network for the Pacific: Construction, calibration, and performance. *J. Atmos. Oceanic Technol.*, **26**, 145–166.
- Tripoli, G.J. and W.R. Cotton, 1986: An intense, quasi-steady thunderstorm over mountainous terrain Part IV: Three-dimensional numerical simulation. *J. Atmos. Sci.*, **43**, 894-913.